

---

---

NUCLEI  
Experiment

---

---

## Investigation of Space-Charge Effects in Gaseous Tritium as a Source of Distortions of the Beta Spectrum Observed in the Troitsk Neutrino-Mass Experiment

A. I. Belesev, E. V. Geraskin, B. L. Zhuikov, S. V. Zadorozhny, O. V. Kazachenko,  
V. M. Kohanuk, N. A. Lihovid, V. M. Lobashev, A. A. Nozik, V. I. Parfenov,  
A. K. Skasyrskaya, E. A. Sudachkov, N. A. Titiov, and V. G. Usanov

*Institute for Nuclear Research, Russian Academy of Sciences,  
pr. Shestidesyatiletiya Oktyabrya 7a, Moscow, 117312 Russia*

Received June 4, 2007; in final form, September 19, 2007

**Abstract**—Results of searches for effects of space-charge accumulation in the gaseous tritium source in the Troitsk neutrino-mass experiment are presented. The broadening and the shift of the  $L3$  line of conversion electrons in a  $^{83m}\text{Kr}$  gaseous source circulating together with tritium was investigated. The attained limit on the magnitude of fluctuations of the space-charge potential makes it possible to set a limit on the negative neutrino mass squared in the Troitsk neutrino-mass experiment ( $-0.8 < \Delta m_\nu^2 \leq 0 \text{ eV}^2$ ), a spurious effect associated with this potential. A statistically reliable shift of the position of the  $L3$  line is discovered. This indicates that processes of space-charge accumulation do indeed proceed in the source at a level that is significant for the future experiment Katrin.

PACS numbers: 23.40.-s

DOI: 10.1134/S1063778808030046

### 1. INTRODUCTION

Searches for a kinematical mass of the neutrino are one of the most important problems in neutrino physics. Although investigations of neutrino oscillations for different neutrino flavors proved that the neutrino mass is nonzero, the issue of its absolute scale remains open. Investigation of the tritium beta-decay spectrum in the vicinity of the endpoint energy by means of an integral electrostatic spectrometer featuring an adiabatic magnetic collimation [1, 2] seems the most promising in this respect.

Troitsk  $\nu$ -mass (neutrino mass) was the first setup of this type. It was designed at the Institute for Nuclear Research (INR, Russian Academy of Sciences, Moscow) [3]. Since 1993, regular measurements of the tritium beta spectrum in the vicinity of the endpoint energy have been performed at this setup with the aim of searches for the electron-antineutrino mass.

The setup comprises an integral electrostatic spectrometer featuring an adiabatic magnetic collimation [4], a windowless gaseous-tritium source (WGTS) of electrons that involves circulating molecular tritium in the gaseous state, a cryogenic system [5] for the superconductor solenoids of the

spectrometer [6], a high-voltage system, and a data-acquisition system [7].

The results obtained in this experiment provide the presently lowest limit on the kinematical mass of the antineutrino in direct beta-decay experiments, the anomaly in the tritium beta-decay spectrum in the vicinity of the endpoint energy being simultaneously taken into account [8–10]. The observed anomaly manifests itself as a steplike structure in the integral beta spectrum, this corresponding to a peak or a monoenergetic line in the differential spectrum. If the anomaly is not taken into account in fitting the experimental spectrum, the squared mass  $m_\nu^2$  appears to be negative. The position of the step with respect to the endpoint energy of the beta-decay spectrum and its absolute height changed from one run to another. The origin of this anomaly, which hinders the determination of the neutrino mass and which causes an approximately twofold increase in the systematic uncertainty, is not clear at the present time.

The results obtained by the Neutrino Mainz group from searches for the neutrino mass in tritium beta decay have been published within the past three years [11]. Some of their measurements were performed simultaneously with those of the Troitsk group

**Table 1.** Parameters of the  $^{83m}\text{Kr}$  conversion line [15]

Level	Line	$E_e$ , eV	$\Gamma_e$ , eV	Intensity, %
$1s_{1/2}$	$K$	$17\,830.0 \pm 1.8$	$2.83 \pm 0.12$	23.8
$2p_{1/2}$	$L2$	$30\,424.4 \pm 3.0$	$1.84 \pm 0.05$	24.5
$2p_{3/2}$	$L3$	$30\,477.2 \pm 3.0$	$1.4 \pm 0.02$	38.1
$3p_{1/2}$	$M2$	$31\,934.2 \pm 3.2$	$1.99 \pm 0.32$	
$3p_{3/2}$	$M3$	$31\,941.9 \pm 3.2$	$1.66 \pm 0.06$	
$4s_{1/2}$	$N1$	$32\,127.8 \pm 3.2$	$0.19 \pm 0.04$	
$4p_{1/2}$	$N2$	$32\,140.9 \pm 3.2$	$0.59 \pm 0.04$	0.38
$4p_{3/2}$	$N3$			0.57

and did not reveal any steplike anomaly. The Neutrino Mainz setup has smaller dimensions than the Troitsk  $\nu$ -mass setup and employs molecular tritium frozen onto a graphite substrate as a source of electrons.

In view of the above facts, it seems necessary to study thoroughly systematic effects associated with WGTS operation. In the present study, we analyze effects of space-charge accumulation that are caused by outgoing fast beta electrons. A nonzero potential of the space charge at the point of tritium decay shifts the observed endpoint energy in the beta spectrum, while the variation of this potential over the source volume leads to the smearing of the endpoint energy. This smearing causes an additional negative shift of the observed neutrino mass squared [12],

$$\Delta m_\nu^2 = -2(\sigma_1^2 + \sigma_2^2 + \sigma_3^2 + \dots), \quad (1)$$

where  $\sigma_i^2$  is the  $i$ th component of the variance of the endpoint energy and  $m_\nu$  is the neutrino mass.

All sources of smearing of the endpoint energy must be taken into account in data processing; otherwise, the experimental result for the neutrino mass squared appears to be shifted to the region of negative values. Variations in the space charge at a level of several eV units in the gaseous source (the respective variance of the endpoint energy is about 5 to 10 eV<sup>2</sup>) could result in a negative mass squared  $m_\nu^2$  at the Troitsk setup without such an effect at the Mainz setup.

Simple estimations demonstrate that the equilibrium concentration of electron-ion pairs is  $10^7 \text{ cm}^{-3}$  in the gaseous source of the Troitsk  $\nu$ -mass setup [13]. With allowance for the source dimensions and the tritium temperature, this suggests the emergence of a low-temperature plasma. The analysis of this plasma is complicated by the presence of a strong magnetic field [14].

The effects of space-charge generation can be studied experimentally if some other radioactive gas that is a source of monoenergetic electrons whose energy is known and is close to the endpoint energy of tritium-beta-decay electrons (about 18 575 eV) is added to the circulating tritium. Since the two gases are distributed similarly over the source volume for a first approximation, variations in the space-charge potential would cause similar broadening of the monoenergetic line, and this broadening is rather easy to record. The metastable isotope  $^{83m}\text{Kr}$ , which has several conversion lines of small width and appropriate energy, is such a gas that possesses unique properties (Table 1).

It should be noted that the  $^{83m}\text{Kr}$ -tritium mixture was used previously in a spectrometer of poorer energy resolution only to determine the line shift—that is, the mean value of the space-charge potential [12].

The  $^{83m}\text{Kr}$  isotope, whose half-life is 1.86 h, is a product of  $^{83}\text{Rb}$  decay (86.2 d). In order to obtain  $^{83}\text{Rb}$ , targets 1.1 g/cm<sup>2</sup> thick were manufactured from a calcined strontium fluoride powder placed into a hermetically sealed stainless-steel container whose walls were 100  $\mu\text{m}$  thick. The atmosphere was inert within the container. The targets were irradiated with protons of energy in the range 120–150 MeV and current up to 6  $\mu\text{A}$  by means the beam channel at the INR Moscow Meson Factory [16]. The target was intensely cooled with water on all sides. The  $^{83}\text{Rb}$  yield was 26  $\mu\text{Ci}/(\mu\text{A h})$  at the end of irradiation. In order to extract  $^{83}\text{Rb}$  from the target, irradiated strontium fluoride was heated in a quartz tube at a temperature of 1200°C in a 150-ml/min helium flow for 4 h, the temperature being raised slowly within the first two hours in order to remove volatile components. The quartz-tube inner surface was covered evenly with graphite insertions in order to prevent an active destruction of quartz and any metals by

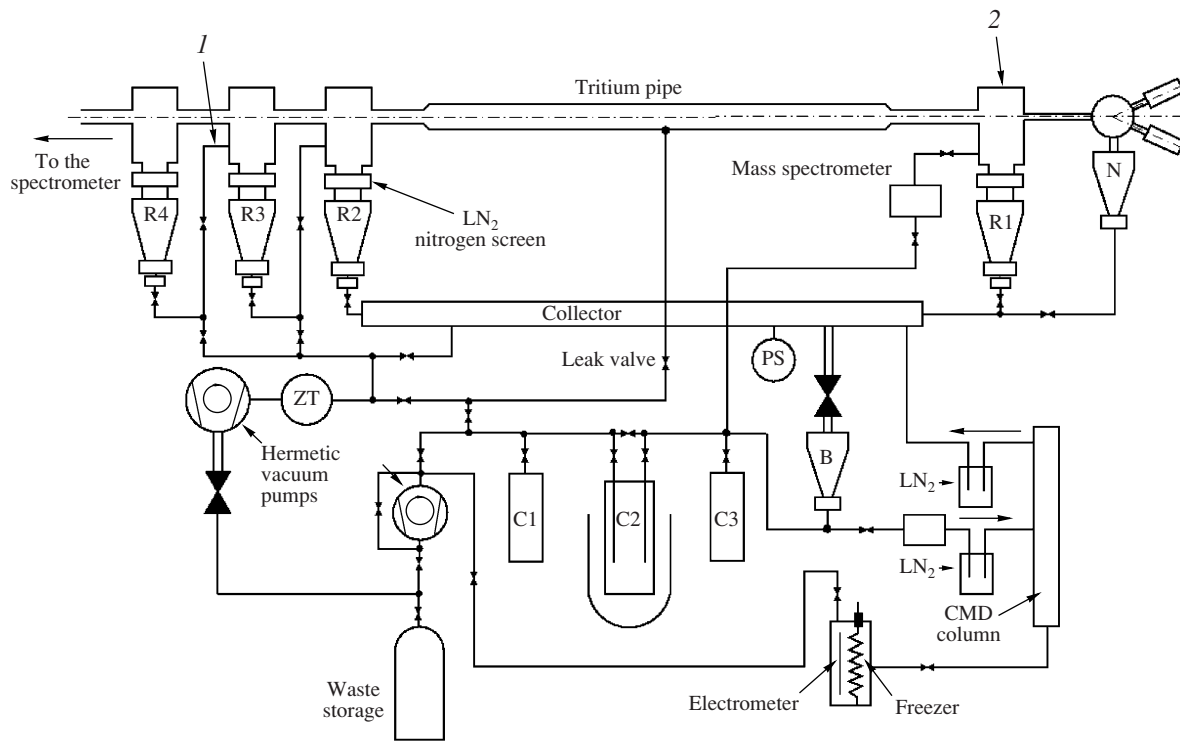


**Fig. 1.** Places of krypton supply to the tritium electron source in (1) Run 39 and (2) Run 40. Here, R1, . . . , R4, B, and N are steam-mercury diffusion pumps; ZT is a zeolite trap; PS is a pressure sensor; C1 is a storage cartridge; C2 is a purifying cartridge; and C3 is a transport container.

evolved HF. Under these conditions, 93% of  $^{83}\text{Rb}$  was sublimated, whereupon it was deposited in the form of a thin layer onto the inner surface of a graphite receiver at the furnace outlet. The graphite receiver was cut and placed into a stainless-steel container connected to the circulating tritium volume of the Troitsk  $\nu$ -mass spectrometer. The rubidium-source activity was up to  $30 \mu\text{Ci}$  at the beginning of the measurements.

The thin rubidium source was heated to  $700^\circ\text{C}$  during the measurements in order to promote krypton release. Since rubidium was deposited onto a high-temperature material whose gas release was low, a direct connection of the source ampule to the tritium volume did not impair a vacuum in the spectrometer. Residual gases in the circulation loop were absorbed in a purifying cartridge also used to purify tritium.

In order to study effects of the space charge at the Troitsk  $\nu$ -mass setup, two measurement runs were performed in November 2004 (Run 39) and June 2005 (Run 40). Each of them took about two weeks, the configuration of the magnetic fields of the spectrometer being different, as well as the places of krypton injection into the source. Technical procedures for adjusting stable krypton circulation and an acceptable counting of krypton in the operating volume of the source consumed most of the run time.

## 2. UPGRADE OF THE SETUP

Initially, we planned to use the  $K$  conversion line of krypton (17.8 keV) in our experiment. However, the counting rate for this line appeared to be overly low (about  $10 \text{ s}^{-1}$ ) in relation to the intensity of the tritium spectrum at this point (about  $10^4 \text{ s}^{-1}$ ). It was impossible to measure precisely the  $K$ -line shape against this background.

More adequate background conditions can be achieved by using conversion lines at energies above the endpoint energy of tritium beta decay. In this case, the background is due exclusively to lines of higher energy. The  $L2$  and  $L3$  lines require the smallest increase in the spectrometer voltage, up to 30.5 kV (Table 1). The  $L3$  line, which provides a signal-to-background ratio of about 2 : 1, was preferred as more intense.

The maximum voltage applied to the spectrometer previously did not exceed 22 kV. We expected that, upon increasing the voltage up to 30.5 kV, there would arise a grave problem of spectrometer instability to a high-voltage discharge in the region of a strong magnetic field. In this connection, about 1.5-fold reduction of the current in the superconductor solenoids of the spectrometer in relation to that used in regular measurements became necessary.

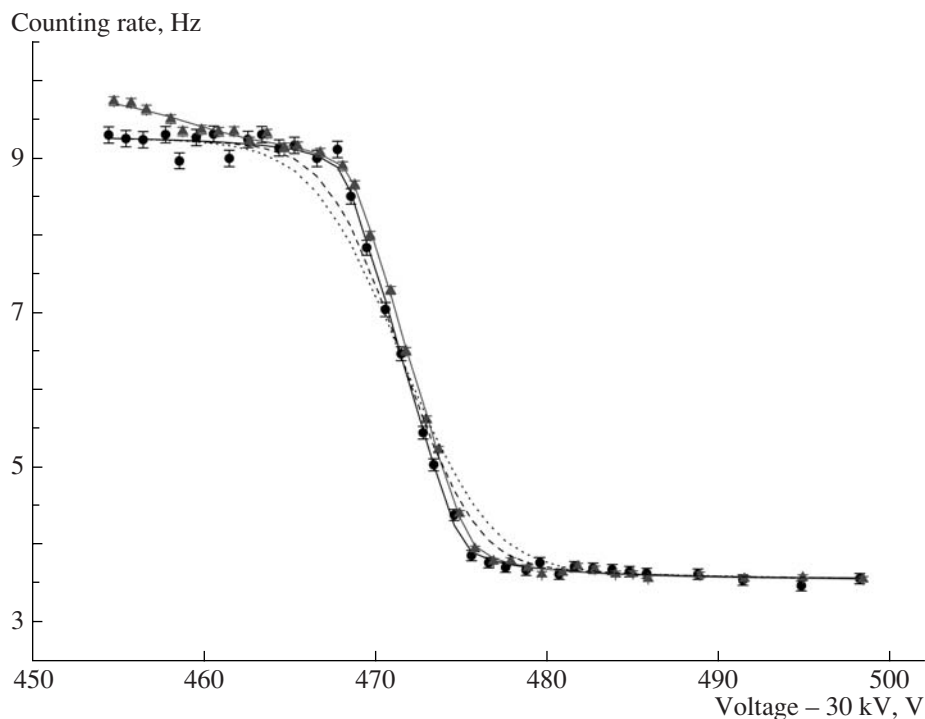


**Fig. 2.** Experimental shape of the  $^{83m}\text{Kr}$   $L3$  conversion line according to measurements in Run 39 with the integral spectrometer for the circulation of (●) pure  $^{83m}\text{Kr}$  and (▲) a mixture of krypton and tritium in the gaseous source. The data obtained with the tritium–krypton mixture at the source thickness of  $X = 0.26$  were normalized to the same intensity of the  $L3$  line undistorted by scattering. The dashed and dotted curves represent the calculated line shape in the case of the source-potential scatter whose variance is 5 and 10  $\text{eV}^2$ , respectively. The spectrometer resolution was 6.8 eV.

Although the reduction of the current caused degradation of the spectrometer resolution, this enabled us to measure the krypton spectrum against a nearly negligible background at an  $L3$ -line intensity of 1 to  $20 \text{ s}^{-1}$ .

An upgrade of the high-voltage system was required for ensuring spectrometer operation at an increased voltage [7]. The manufacturer (VIVN Ltd.) raised the output voltage of the high-voltage sources to 35 kV and developed a new remote-control system. The configuration of the high-voltage divider was also changed in Run 40 for the voltage measured with the precision voltmeter Solartron 7061 to be within its most precise operating range of 10 V.

At first, the differential-pumping port P3 (point 1 in Fig. 1) was chosen for krypton supply to the circulation loop of the gaseous source. However, the intensity of the krypton line in the circulation regime proved to be considerably smaller than the calculated intensity. In performing the next measurement run, we changed the place of krypton supply, arranging it in the region of intermediate pressure in the source portion opposite to the spectrometer (point 2 in Fig. 1).

The intensity was approximately equal in the two runs. In Run 40, the whole amount of rubidium was

placed in a single ampule, but this only enabled us to compensate for the decrease in the intensity because of  $^{83}\text{Rb}$  decay.

### 3. MEASUREMENT PROCEDURE

The observed line had a steplike shape (Fig. 2), its descending-portion width being equal to the spectrometer resolution  $\Delta E/eU_0 = H_{\min}/H_{\max}$ . The sum of the scattered magnetic field of the superconductor solenoids,  $H_{\text{cold}}$ , and the field of the warm solenoid,  $H_{\text{warm}}$ , forms the main part of the field  $H_{\min}$  in the analyzing plane of the spectrometer; by  $H_{\max}$ , we denote the field at the center of the entrance superconductor solenoid. The currents in the cold and warm solenoids were maintained at a constant level to within one percent. Up to 45 high-voltage values with a step of 1 V were chosen for the measurements. These points covered completely the  $L3$ -line portion not distorted by scattering and the background region. The  $L2$  conversion line was observed simultaneously with the  $L3$  line in Run 39.

The measurement time was 10 s at each high-voltage value, and the time of switching between the points was about 5 s. Each scan over all points was saved in a separate file. The measurements were

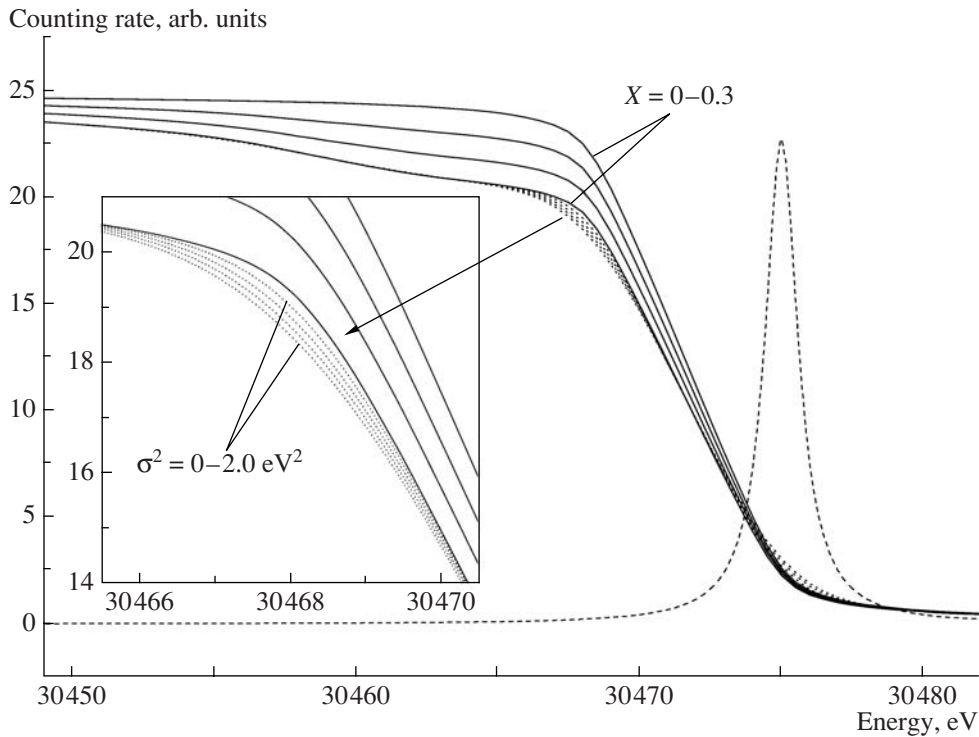


**Fig. 3.** Effect of different parameters on the shape of the observed integral spectrum of the  $L3$  line: (dashed curve) original conversion line of width 1.4 eV, (solid curves) integral-spectrometer response at a resolution of 6.8 eV and a source thickness of  $X = 0$  (pure krypton) or 0.1 to 0.3 (krypton–tritium mixture), and (dotted curves) effect of line broadening at  $\sigma^2 = 0$ – $2.0 \text{ eV}^2$ .

performed in direct and in inverse order for the same sequence of points. Tritium was added to the source one to two times a day in order to compensate for the first-order drift.

In choosing the current in the warm solenoid, we had to compromise between the stability of background conditions in the spectrometer, this requiring an increase in the warm-solenoid current, and the optimization of the spectrometer resolution, this requiring a reduction of the current. The measurements were performed with a current of 25 and 15 A in the warm solenoid in Run 39 and only with a current of 15 A current in Run 40 (this enabled us to improve the resolution from 8.2 to 6.8 eV). The temperature of the source tritium pipe was 110 K in both runs, which was above that of the tritium pipe in the investigation of the tritium beta spectrum, 28 K, since a strong temperature dependence of the source intensity was established. At lower temperature, krypton began to freeze out onto the walls of the source tritium pipe and then onto the liquid-nitrogen traps of the mercury pumps.

Tritium density in the source was within the range  $(2.0\text{--}3.0) \times 10^{14}$  molecule/cm<sup>3</sup> in Run 39 and was  $1.7 \times 10^{14}$  molecule/cm<sup>3</sup> in Run 40; according to [17], this is equivalent to, respectively, 0.17 and

0.12 of the mean free path of 30.5-keV electrons with respect to inelastic scattering on a tritium molecule.

#### 4. EXPERIMENTAL-DATA PROCESSING

The results obtained at identical sampling conditions were summed. For the  $L3$  line, we ultimately had pairs of data samples differing only by the presence or absence of tritium in the gaseous source. In addition to line broadening, which we intended to estimate, tritium supply to the source caused sizable inelastic scattering of electrons.

In describing the shape of the  $L3$  conversion line, we used the Lorentz distribution

$$L(E, E_e, \Gamma_e) = \frac{\Gamma_e}{2\pi} \frac{1}{(E - E_e)^2 + \Gamma_e^2/4}, \quad (2)$$

where  $E$  is the electron energy, and  $E_e$  and  $\Gamma_e$  are, respectively, the position and the width of the conversion line.

The line broadening caused by the space-charge effect and some random factors was assumed to have a Gaussian shape,

$$G(\delta E, \sigma^2) = \frac{1}{\sqrt{2\pi}\sigma} e^{-\delta E^2/(2\sigma^2)}, \quad (3)$$

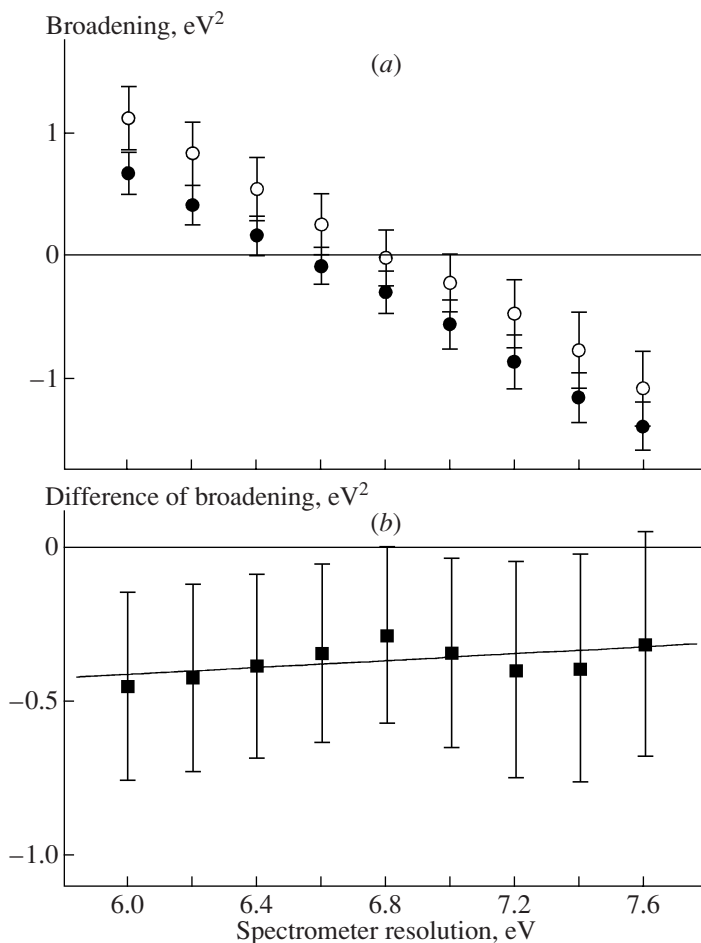


**Fig. 4.** (a) Fitting of  $L3$ -line broadening in Run 40 versus the presumed value of the spectrometer resolution: (○) pure krypton circulation and (●) circulation of a krypton–tritium mixture. (b) Difference of line-broadening values from Fig. 4a: (■) net effect of the presence of tritium in the gaseous source.

where  $\delta E$  and  $\sigma^2$  are, respectively, the energy shift and its variance. The energy spectrum of electrons that traversed the source is determined by the probability of multiple inelastic scattering and by the spectra of the corresponding energy losses; that is,

$$S(\Delta E) = P_0\delta(\Delta E) + P_1S_1(\Delta E) + P_2S_2(\Delta E) + \dots, \quad (4)$$

where  $\Delta E$  is the energy lost by an electron; the delta function  $\delta(\Delta E)$  is the spectrum of electrons

that did not undergo scattering;  $S_1(\Delta E)$  is the spectrum of electrons from a single-inelastic-scattering event [9];  $S_2(\Delta E) = S_1(\Delta E) \otimes S_1(\Delta E)$  is the spectrum of electrons from a double-inelastic-scattering event; and  $P_k$  is the average of the probability for the  $k$ -fold inelastic scattering of electrons in the source over the depth and emission angle,

$$P_k = \left\langle \frac{(x/\cos\theta)^k}{k!} \exp(-x/\cos\theta) \right\rangle_{k,\cos\theta}. \quad (5)$$

In (5),  $x$  is the current coordinate,  $0 < x < X$ , where  $X$  is the source thickness expressed in units of the electron mean free path:

$$X = \sigma_{\text{inel}} \int n(x) dx. \quad (6)$$

Here,  $\sigma_{\text{inel}}$  is the cross section for inelastic scattering and  $n(x)$  is the number of molecules per cubic centimeter.

The ratio of the number of electrons recorded by the spectrometer to the total number of elec-

**Table 2.** Parameters of the optimum fit

Run ( $I_{\text{cold}}/I_{\text{warm}}$ )	Spectrometer resolution, eV	Source thickness, $X$
40 (100 A/15 A)	$6.65 \pm 0.20$	$0.125 \pm 0.035$
39 (100 A/15 A)	$7.14 \pm 0.28$	$0.262 \pm 0.027$
39 (100 A/25 A)	$8.19 \pm 0.16$	$0.18 \pm 0.02$

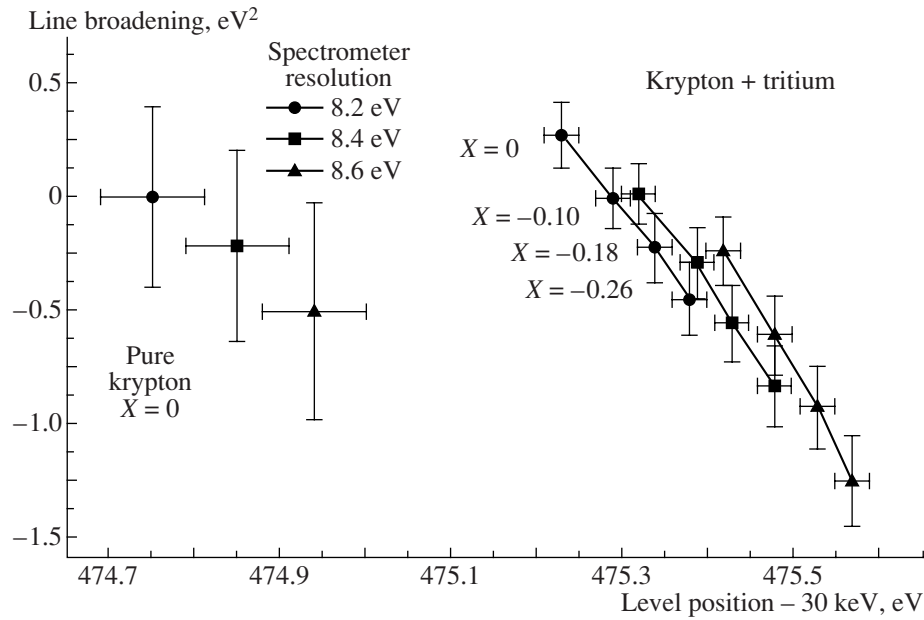


Fig. 5. Analysis of data obtained in Run 39 (100 A/25 A). For the case where a krypton–tritium mixture circulates, different values assumed for the spectrometer resolution lead to a similar shift of the fitted parameters of the  $L3$  line.

trons that traversed the strong-field region—that is, electrons produced within the solid angle  $\Omega_{\text{source}} = \pi(H_{\text{source}}/H_{\text{max}})$ —depends on the excess of their energy  $E$  over the spectrometer potential  $eU_0$ . This electron fraction is described by the spectrometer transmission function

$$\text{Res}(E - eU_0) \quad (7)$$

$$= \begin{cases} 0 & \text{for } E - eU_0 < 0, \\ (E - eU_0)/\Delta E & \text{for } 0 < E - eU_0 < \Delta E, \\ 1 & \text{for } \Delta E < E - eU_0, \end{cases}$$

where  $\Delta E = eU_0(H_{\text{min}}/H_{\text{max}})$  is the spectrometer resolution.

The observed electron spectrum  $N(E)$  is obtained as the convolution of the above functions:

$$N(E, \sigma^2, X, \dots) = \text{Res} \otimes S \otimes G \otimes L. \quad (8)$$

Here, it is natural to use the normalization condition  $N(E) = 1$  for  $E \rightarrow -\infty$  (the condition  $N(E) = 0$  for  $E \rightarrow +\infty$  holds automatically). Figure 3 shows the dependence of the line shape on some experimental parameters.

A unidirectional change in the counting rate with increasing smearing parameter  $\sigma^2$  is a significant feature of the spectra presented here. By way of example, we indicate that, at 30 465 eV, the greater the smearing, the more pronounced the decrease in the counting rate. If one seeks small deviations of the parameter  $\sigma^2$  from zero, it is important to interpret properly statistical deviations of the counting rate in

the opposite direction (growth of the counting rate in the above example). It is necessary to define a continuation of the function  $N(E, \sigma^2, \dots)$  to the region  $\sigma^2 < 0$  in such a way that statistical fluctuations of the counting rate do not bias the estimate of  $\sigma^2$ . The following formula provides satisfactory results:

$$N(E, \sigma^2 < 0) = N(E, \sigma^2 = 0) - (N(E, |\sigma^2|) - N(E, \sigma^2 = 0)). \quad (9)$$

We note that it is precisely  $\sigma^2$  (not  $\sigma$ ) that obeys approximately a normal distribution in data processing. It is difficult to compare directly the spectra taken for pure krypton with those taken for its mixture with tritium since the flat spectrum portion develops a slope because of inelastic losses if tritium is present in the source, while the total counting rate increases. Therefore, the pair spectra were processed independently, whereupon the resulting parameter values were compared.

In order to analyze the spectra, we modified the  $\chi^2$ -minimization code based on the MINUIT package [18] and applied previously in handling data from neutrino-mass searches. We fitted (i) the amplitude of the spectrum (step height), (ii) the magnitude of the energy-independent background, (iii) the krypton-line position, and (iv) the krypton-line broadening.

The spectrometer resolution and the source thickness were constant in fitting the data measured with tritium. The  $L3$ -line width was taken from [15] and was not varied either.

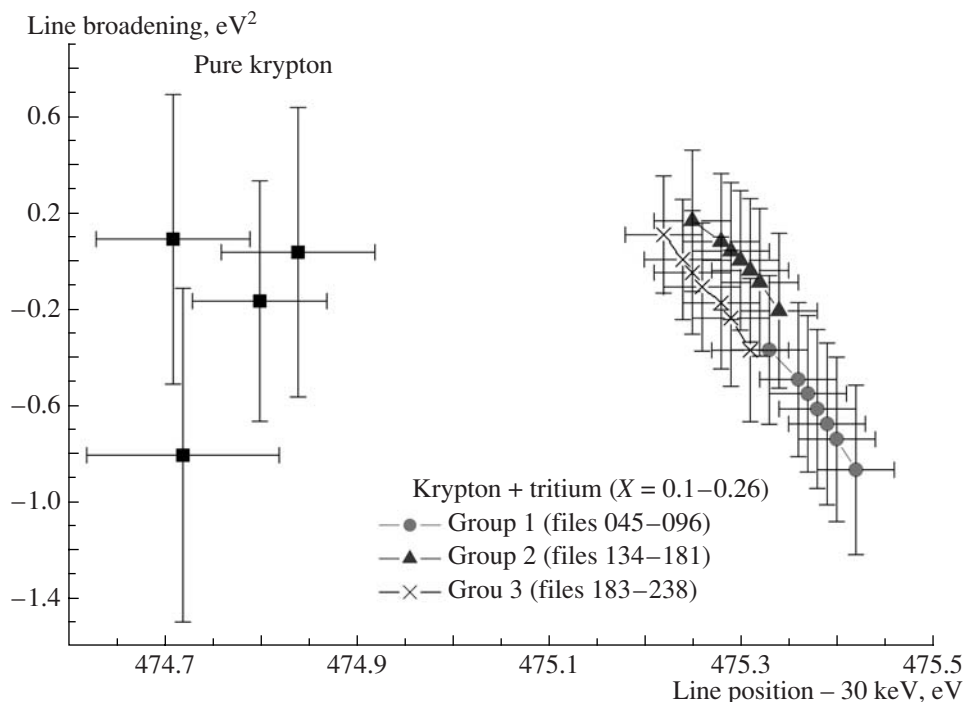


**Fig. 6.** Illustration of the results obtained in Run 39 (100 A/25 A) at a resolution of 8.2 eV. Data on pure-krypton circulation were divided into four subgroups (two of them were taken at the beginning of the measurements, while the other two were taken at their end); data on the circulation of a tritium–krypton mixture were divided into three subgroups.

Previously, the resolution function was determined with the aid of an electron gun. In the present experiment, this appeared to be impossible because of special features of the gun designed to be operated at a lower voltage. At the first stage, the spectra obtained with pure krypton were therefore fitted at several values of the spectrometer resolution, whereby its optimum value and its variance were found by requiring minimum  $\chi^2$  and the shift of  $\Delta\chi^2 = +1$ , respectively.

At the second stage, the spectra obtained with a krypton–tritium mixture were processed by using the detector resolution determined at the first stage and various values of the source thickness  $X$ , and the optimum value of this thickness and its variance were found in a similar way. The results of this data processing are compiled in Table 2.

Thus, we obtained the position and the broadening of the pure-krypton line at the first stage and their counterparts for the tritium–krypton mixture at the second stage. The correlations with the source thickness appeared to be small, but the correlations with the spectrometer resolution were dominant in the total uncertainty (Fig. 4a).

It should be emphasized that the resolution is determined by the ratio of the field (current) in the warm solenoid to the scattered field (current) in the cold solenoid (to a precision of about 1%) and that the gas

distribution over the source cross section is identical (to a precision of about  $10^{-3}$ ). Therefore, the true resolution value is the same in the two measurements, and the uncertainty of its absolute value can be taken into account in the differences of the broadening and position values, which are virtually independent of the resolution value (see Fig. 4b). The statistical uncertainty is dominant in the total uncertainty if the data are handled in the way outlined above.

It seems that the description used was not absolutely adequate, with the result that the broadening parameter  $\sigma^2$  was shifted to the region of negative values in the analysis of the pure-krypton spectra. The intrinsic  $L3$ -line width or the spectrometer resolution can be varied in order to eliminate this effect. It is worth noting that the shift of the broadening does not change considerably in this case.

## 5. RESULTS OF THE ANALYSIS

Our analysis of the data obtained in Run 39 (100 A/25 A) at the cold- and warm-solenoid currents of 100 A and 25 A, respectively, did not reveal any sizable broadening of the  $^{83m}\text{Kr}$  line in the presence of tritium in the mixture, but it showed a shift of the line position. Figure 5 displays the calculated broadening of the line and its position for three values of the spectrometer resolution (Table 2) and four

**Table 3.** Results of data processing

Measurement run	Broadening $\Delta\sigma^2$ , eV <sup>2</sup>	Shift $\Delta E_0$ ( $\pm$ syst.), eV
40 (100 A/15 A)	$-0.28 \pm 0.30$	$0.193 \pm 0.051$ ( $\pm 0.011$ )
39 (100 A/25 A)	$-0.24 \pm 0.45$	$0.59 \pm 0.065$ ( $\pm 0.014$ )
39 (100 A/15 A)	$0.32 \pm 0.30$	$0.42 \pm 0.060$ ( $\pm 0.014$ )

**Table 4.** Comparison of measurement conditions and results in different experiments

Experiment	Source length, m	Source diameter, cm	Magnetic field, kG	Temperature, K	Source thickness, $10^{17}$ mol/cm <sup>-2</sup>	Shift of <sup>83m</sup> Kr line, eV
LANL (Los Alamos)	3.7	3.8	3.1	160	0.07	<0.5
INR (Troitsk), regular measurements	1–3–1	2.0–5.0–2.0	37–5.6–37	30	1.0	
INR (Troitsk), measurements with krypton	1–3–1	2.0–5.0–2.0	25–3.7–25	110	0.35–0.50	0.2–0.6
FZK (Karlsruhe), KATRIN project	10.0	9.0	50.0	30	5.0	

values of the thickness  $X$  (those from Table 2 and  $X = 0$ ). It is evident that a variation in the assumed spectrometer resolution leads to a parallel shift of the graphs, changing the estimate of the shift parameters in the presence of tritium only slightly. The source thickness has only a small effect on the results even if  $X = 0$ .

The data sample obtained with a krypton–tritium mixture was broken down into three portions in order to test the statistical properties of the results. The measurements with pure krypton were performed at the beginning and at the end of the experiments, both data samples being separated into two groups. The measurements with a krypton–tritium mixture were performed continuously, and the resulting data were separated into three groups with respect to time. Figure 6 demonstrates the stability of the observed shift of the line and the absence of its broadening.

Similar results were obtained by using grouped data from Run 39 (100 A/15 A) and Run 40. The results of the analysis are compiled in Table 3. The uncertainties in the calculated broadening and shift are determined by the statistical scatter. In calculating the shift, the systematic uncertainties caused by the uncertainty in the values of the spectrometer resolution and the source thickness amounted to less than 25% of the statistical uncertainties.

The variations in the line position in the different measurements differed markedly from one another;

however, a comparison of the data in Tables 2 and 3 revealed no correlations with the source thickness. The observed scatter is likely to be associated with some other parameter, which could not be revealed because of insufficient statistics.

## 6. DATA REPROCESSING

A new code based on the method of quasioptimal moments [19] was used to verify the results of our data analysis. A new set of parameters involving the setup resolution and an analog of the effective source thickness was used in data reprocessing (all of the parameters were fitted simultaneously).

The results of this reprocessing are by and large in agreement with the previous results. The line broadening is close to zero in all data samples, while the shift is obviously positive. The precise shift values obtained in Run 39 are in good agreement with those obtained previously. The shift appeared to be somewhat greater in Run 40, but this can be explained by the use of a different parameter set and by allowance for the effect of the resolution.

We have calculated the spectrometer resolution by tracking particles, taking into account the space nonuniformity of the electric and magnetic fields. The resulting averaged values reproduce the experimental data and explain them.

## 7. CONCLUSIONS

An estimate of the possible space-charge-induced correction to the neutrino mass in the Troitsk  $\nu$ -mass experiment has been obtained. From a treatment of data on the broadening of the  $L3$  conversion-electron line of the  $^{83m}\text{Kr}$  source, it has been found that the variance of the electric potential in the gaseous-source volume does not exceed  $0.4 \text{ eV}^2$ , which constrains the negative shift of the measured square of the neutrino mass to be within the range  $-0.8 < \Delta m_\nu^2 \leq 0 \text{ eV}^2$ . It should be noted that the measurements have been performed at a temperature higher by a factor of 3.5 and the source thickness smaller by a factor of 2 to 3 than in the usual measurements of the neutrino mass at the Troitsk  $\nu$ -mass setup (Table 4). Simple considerations [14] give every reason to hope that, in measuring the neutrino mass at the Troitsk  $\nu$ -mass setup, a higher density and a lower temperature of the neutral gas result in a lower electron-gas temperature, which determines the scale of plasma effects in the gaseous source. Thus, the constraints set here on the variance of the space-charge potential provide an upper limit on the corresponding spurious effect in the Troitsk  $\nu$ -mass experiment, and the anomaly observed in the vicinity of the endpoint energy in the tritium beta spectrum [8–10] cannot be due to plasma effects in the tritium source.

A statistically significant shift of the  $L3$ -line position (Fig. 2) has been found in the case where the source pipe was filled with the isotope  $^{83m}\text{Kr}$  and tritium simultaneously. This indicates that processes of space-charge accumulation do indeed occur in the source at a level significant for the future joint experiment KATRIN. It is necessary to ensure two orders of magnitude more stringent constraints on the magnitude of spurious effects for  $m_\nu^2$  in order to achieve the goal announced for the KATRIN experiment.

Unexpectedly, the electron energy is shifted in the positive direction in the presence of tritium—that is, the source is charged negatively, which is at odds with the usual concept of plasma formation. No explanation for this phenomenon has so far been found, and further studies are required to clarify it.

Unfortunately, a reliable rescaling of the observed space-charge effects for other source parameters—in particular, for those of the gaseous source in the KATRIN setup—is hampered by the complexity of processes in tritium plasma. It is desirable to study experimentally the dependence of the shift and the broadening of the  $^{83m}\text{Kr}$  line on the basic source parameters to a considerably higher degree of precision. At present, the spectrometer is being upgraded with the aim of significantly increasing (by a factor of about

two) its resolution and improving its sensitivity by enlarging its central part.

## ACKNOWLEDGMENTS

We are grateful to A.A. Golubev, S.A. Osipov, I.I. Palamarchuk, and A.A. Stepanov for their assistance in performing the measurement runs, to A.I. Egorov (Petersburg Nuclear Physics Institute, PNPI) for developing procedures for the extraction of rubidium, and to V.A. Nikitin (VIVN Ltd.) for developing upgraded high-voltage sources.

This work was supported by the Russian Federal Atomic Energy Agency and the Russian Foundation for Basic Research (project no. 05-02-17238); it is one of the phases of the KATRIN project realization.

## REFERENCES

1. Ch. Weinheimer, *Int. J. Mod. Phys. A* **21**, 1875 (2006).
2. J. Angril et al., Preprint No. 7090, FZKA (Karlsruhe, 2005).
3. V. M. Lobashev and P. E. Spivak, Preprint No. P-0291, IYAI AN SSSR (Institute for Nuclear Research, USSR Academy of Sciences, Moscow, 1983).
4. S. N. Balashov et al., Preprint No. P-0617, IYAI AN SSSR (Institute for Nuclear Research, USSR Academy of Sciences, Moscow, 1989).
5. A. I. Belesev et al., Preprint No. P-0614, IYAI AN SSSR (Institute for Nuclear Research, USSR Academy of Sciences, Moscow, 1988).
6. A. I. Belesev et al., Preprint No. P-0615, IYAI AN SSSR (Institute for Nuclear Research, USSR Academy of Sciences, Moscow, 1989).
7. A. I. Berlev et al., Preprint No. P-1103/2003, IYAI RAN (Institute for Nuclear Research, Russian Academy of Sciences, Moscow, 2003).
8. A. I. Belesev et al., *Phys. Lett. B* **350**, 263 (1995).
9. V. M. Lobashev et al., *Nucl. Phys. A* **654**, 982 (1999).
10. V. M. Lobashev et al., *Phys. Lett. B* **460**, 227 (1999).
11. C. Kraus et al., hep-ex/0412056.
12. R. G. H. Robertson and D. Knapp, *Annu. Rev. Nucl. Part. Sci.* **38**, 185 (1988).
13. N. A. Titov (for the KATRIN Collab.), *Phys. At. Nucl.* **67**, 1953 (2004).
14. A. F. Nastoyashchii et al., *Fusion Sci. Techn.* **48** (1), 743 (2005).
15. A. Picard, *Z. Phys. A* **342**, 71 (1992).
16. B. L. Zhuikov et al., *Nucl. Instrum. Methods Phys. Res. A* **438**, 173 (1999).
17. V. N. Aseev et al., *Eur. Phys. J. D* **10**, 39 (2000).
18. F. James, MINUIT, CERN Program Library Long Writeup D 506 (CERN, Geneva, 1998).
19. F. V. Tkachov, physics/0604127.

*Translated by E. Kozlovsky*